ISSN 1007-9327 (print)
ISSN 2219-2840 (online)

World Journal of *Gastroenterology*

World J Gastroenterol 2024 September 28; 30(36): 4014-4082

Published by Baishideng Publishing Group Inc

World Journal of Gastroenterology

Contents

Weekly Volume 30 Number 36 September 28, 2024

EDITORIAL

ORIGINAL ARTICLE

Retrospective Study

Basic Study

CASE REPORT

LETTER TO THE EDITOR

World Journal of Gastroenterology

Weekly Volume 30 Number 36 September 28, 2024

Contents

NAME OF JOURNAL
World Journal of Gastroenterology

ISSN
ISSN 1007-9327 (print) ISSN 2219-2840 (online)

LAUNCH DATE
October 1, 1995

FREQUENCY
Weekly

EDITORS-IN-CHIEF
Andrzej S Tarnawski

EXECUTIVE ASSOCIATE EDITORS-IN-CHIEF
Jian-Gao Fan (Chronic Liver Disease)

EDITORIAL BOARD MEMBERS
http://www.wjgnet.com/1007-9327/editorialboard.htm

PUBLICATION DATE
September 28, 2024

PUBLISHING PARTNER
Shanghai Pancreatic Cancer Institute and Pancreatic Cancer Institute, Fudan University
Biliary Tract Disease Institute, Fudan University

INSTRUCTIONS TO AUTHORS
https://www.wjgnet.com/bpg/gerinfo/204

GUIDELINES FOR ETHICS DOCUMENTS
https://www.wjgnet.com/bpg/GerInfo/287

GUIDELINES FOR NON-NATIVE SPEAKERS OF ENGLISH
https://www.wjgnet.com/bpg/gerinfo/240

PUBLICATION ETHICS
https://www.wjgnet.com/bpg/GerInfo/288

PUBLICATION MISCONDUCT
https://www.wjgnet.com/bpg/gerinfo/208

POLICY OF CO-AUTHORS
https://www.wjgnet.com/bpg/GerInfo/310

ARTICLE PROCESSING CHARGE
https://www.wjgnet.com/bpg/gerinfo/242

STEPS FOR SUBMITTING MANUSCRIPTS
https://www.wjgnet.com/bpg/GerInfo/239

ONLINE SUBMISSION
https://www.f6publishing.com

PUBLISHING PARTNER's OFFICIAL WEBSITE
https://www.shca.org.cn
https://www.zs-hospital.sh.cn

World Journal of Gastroenterology

Submit a Manuscript: https://www.f6publishing.com

World J Gastroenterol 2024 September 28; 30(36): 4044-4056

DOI: 10.3748/wjg.v30.i36.4044

ISSN 1007-9327 (print) ISSN 2219-2840 (online)

ORIGINAL ARTICLE

Retrospective Study

Computed tomography-based multi-organ radiomics nomogram model for predicting the risk of esophagogastric variceal bleeding in cirrhosis

Yu-Jie Peng, Xin Liu, Ying Liu, Xue Tang, Qi-Peng Zhao, Yong Du

Specialty type: Gastroenterology and hepatology

Provenance and peer review: Unsolicited article; Externally peer reviewed.

Peer-review model: Single blind

Peer-review report's classification

Scientific Quality: Grade B, Grade C

Novelty: Grade B, Grade B

Creativity or Innovation: Grade B, Grade B

Scientific Significance: Grade B, Grade B

P-Reviewer: Bi X; Chen W

Received: July 2, 2024

Revised: August 28, 2024

Accepted: September 3, 2024

Published online: September 28, 2024

Processing time: 79 Days and 20 Hours

Yu-Jie Peng, Xin Liu, Ying Liu, Xue Tang, Qi-Peng Zhao, Yong Du, Department of Radiology, The Affiliated Hospital of North Sichuan Medical College, Nanchong 637000, Sichuan Province, China

Yu-Jie Peng, Xin Liu, Department of Radiology, The People's Hospital of Chongqing Liang Jiang New Area, Chongqing 401121, China

Corresponding author: Yong Du, MD, Professor, Department of Radiology, The Affiliated Hospital of North Sichuan Medical College, No. 1 Maoyuannan Road, Nanchong 637000, Sichuan Province, China. duyong@nsmc.edu.cn

Abstract

BACKGROUND

Radiomics has been used in the diagnosis of cirrhosis and prediction of its associated complications. However, most current studies predict the risk of esophageal variceal bleeding (EVB) based on image features at a single level, which results in incomplete data. Few studies have explored the use of global multi-organ radiomics for non-invasive prediction of EVB secondary to cirrhosis.

AIM

To develop a model based on clinical and multi-organ radiomic features to predict the risk of first-instance secondary EVB in patients with cirrhosis.

METHODS

In this study, 208 patients with cirrhosis were retrospectively evaluated and randomly split into training (n = 145) and validation (n = 63) cohorts. Three areas were chosen as regions of interest for extraction of multi-organ radiomic features: The whole liver, whole spleen, and lower esophagus–gastric fundus region. In the training cohort, radiomic score (Rad-score) was created by screening radiomic features using the inter-observer and intra-observer correlation coefficients and the least absolute shrinkage and selection operator method. Independent clinical risk factors were selected using multivariate logistic regression analyses. The radiomic features and clinical risk variables were combined to create a new radiomics-clinical model (RC model). The established models were validated using the validation cohort.

RESULTS
The RC model yielded the best predictive performance and accurately predicted the EVB risk of patients with cirrhosis. Ascites, portal vein thrombosis, and plasma prothrombin time were identified as independent clinical risk factors. The area under the receiver operating characteristic curve (AUC) values for the RC model, Rad-score (liver + spleen + esophagus), Rad-score (liver), Rad-score (spleen), Rad-score (esophagus), and clinical model in the training cohort were 0.951, 0.930, 0.801, 0.831, 0.864, and 0.727, respectively. The corresponding AUC values in the validation cohort were 0.930, 0.886, 0.763, 0.792, 0.857, and 0.692.

CONCLUSION
In patients with cirrhosis, combined multi-organ radiomics and clinical model can be used to non-invasively predict the probability of the first secondary EVB.

Key Words: Artificial intelligence; Cirrhosis; Radiomics; Esophagogastric variceal bleeding

Core Tip: Based on enhanced computed tomography images of patients with cirrhosis and independent clinical risk factors, we developed a new multi-organ combined radiomic model to predict the risk of esophageal variceal bleeding (EVB) in cirrhotic patients, and analyzed its reproducibility and clinical applicability. This new multi-organ combined prediction model can effectively predict the risk of secondary EVB in cirrhosis and provide some support for patient individualized treatment.

Citation: Peng YJ, Liu X, Liu Y, Tang X, Zhao QP, Du Y. Computed tomography-based multi-organ radiomics nomogram model for predicting the risk of esophagogastric variceal bleeding in cirrhosis. *World J Gastroenterol* 2024; 30(36): 4044-4056
URL: https://www.wjgnet.com/1007-9327/full/v30/i36/4044.htm
DOI: https://dx.doi.org/10.3748/wjg.v30.i36.4044

INTRODUCTION

Liver cirrhosis is the late stage of several acute and chronic liver diseases and is currently the eleventh most prevalent cause of mortality globally. Up to 1 million cirrhosis-related deaths are reported annually, accounting for about 2.4% of all global deaths, with more men than women succumbing to the disease[1,2]. The common causes of liver cirrhosis include viral infection, alcoholic liver disease, non-alcoholic fatty liver disease, autoimmune liver disease, long-term cholestasis, drug or toxic substance damage, liver blood circulation disturbance, genetic and metabolic diseases, and parasitic infections[3,4]. The progression of liver cirrhosis is primarily divided into compensatory and decompensated stages. Compensated cirrhosis is mainly characterized by decreased liver function. During the decompensation period, there are many complications such as esophageal variceal bleeding (EVB), spontaneous bacterial peritonitis, hepatic encephalopathy, hepatorenal syndrome, portal vein thrombosis (PVT), and primary hepatic carcinoma[1,4-6]. The most common complication is esophagogastric varices (EV)[7]. According to earlier research, EV is present in around 50% of patients with cirrhosis, and a fatal complication of cirrhotic portal hypertension is EVB. The mortality rate of the first secondary acute EVB can reach up to 15%-20%. Patients who have not received treatment after the first bleeding have a greater than 60% risk of rebleeding within 1 year, and the mortality rate of rebleeding is approximately 20%-33%[8-10]. Owing to the high incidence and mortality rates of EVB, early prediction of the first secondary EVB in patients with cirrhosis is important, especially in those who already carry a high risk of bleeding.

In patients with cirrhosis, endoscopy examination is considered the golden standard for assessing the severity of EV and for making an initial prognosis of EVB risk[1]. However, endoscopy is invasive, and patients with severe underlying diseases, such as cardiovascular disease, hypertension, and acute inflammation, may be unable to tolerate the examination. Further, painless endoscopy carries the risk of general anesthesia, and the endoscopic risk factors depend on the experience and subjectivity of the operator[5]. Contrast-enhanced computed tomography (CT) can be used to effectively evaluate and diagnose EV; however, its success depends on the experience and skill of the radiologists, and a large amount of information in CT images cannot be gleaned through direct human observation. Therefore, developing a non-invasive method for predicting EVB remains essential. However, a standardized diagnostic method for non-invasive prediction of EVB in patients with liver cirrhosis does not exist.

Radiomics is a new approach that extracts all the information contained in the image and then makes a comprehensive and systematic analysis[11,12]. Previous studies have demonstrated promising results of radiomics in predicting EVB[13-17]. However, these studies mainly included features from only a portion of the liver and/or portions of the spleen or esophagus and analyzed single- and multi-level images (*e.g.*, hilar of the liver or hilum of the spleen). Furthermore, there are no noninvasive diagnostic criteria for predicting EVB in the context of cirrhosis. Moreover, previous studies have confirmed the feasibility and important value of multi-organ radiomics analysis[18-20]. Therefore, our study aimed to develop and verify a new multi-organ radiomics model for predicting secondary EVB in patients with cirrhosis by seg-

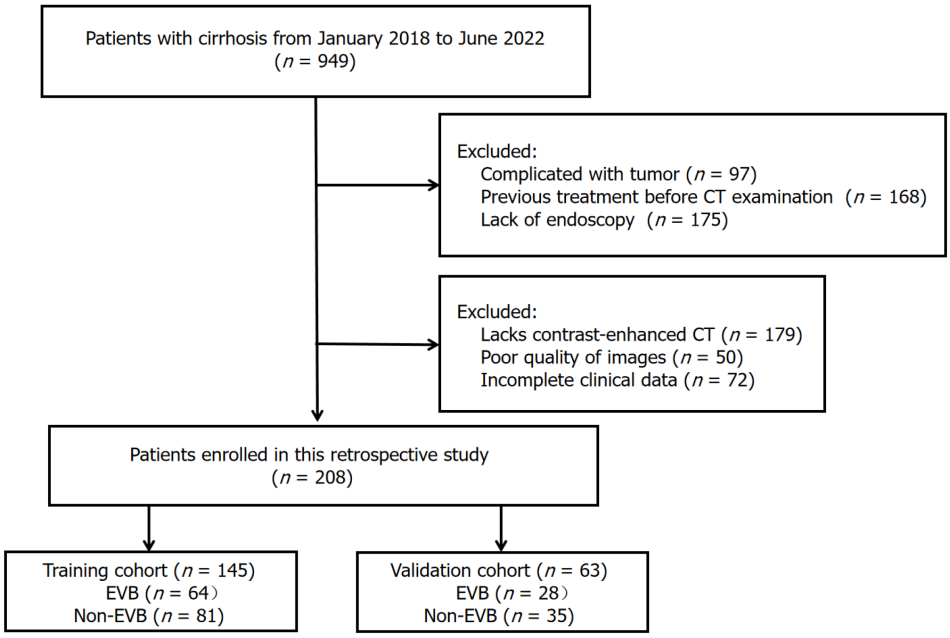

Figure 1 Flowchart of inclusion and exclusion criteria. CT: Computed tomography; EVB: Esophageal variceal bleeding.

menting 3D images of the whole liver, whole spleen, and esophagogastric fundus. To achieve our aim, radiomic features extracted from portal phase-enhanced CT images were combined with clinical features to generate various prediction models.

MATERIALS AND METHODS

Patients

The appropriate institution's medical ethics committee approved this retrospective study.

A retrospective analysis was conducted on the data of 208 patients with liver cirrhosis selected from 949 patients from January 2018 to June 2022. The training (n = 145) and validation (n = 63) cohorts were randomly divided at a ratio of 7:3 (Figure 1). The following inclusion criteria were applied: (1) Diagnosis of cirrhosis based on pathological findings and/or imaging findings and laboratory results; (2) Abdominal contrast-enhanced CT performed within 2 weeks of diagnosis; and (3) Completion of upper gastrointestinal endoscopy. The following exclusion criteria were applied: (1) Presence of tumors in the liver, spleen, and/or esophagus; (2) Previous endoscopic therapy, β-blocker therapy, transjugular intrahepatic portosystemic shunt, splenic embolization, splenectomy, hepatectomy, or other surgeries; (3) Poor-quality or missing CT images; (4) Imperfect clinical data; and (5) Upper gastrointestinal bleeding caused by gastroduodenal ulcer bleeding, hematological diseases, or other primary diseases.

Endoscopic examination and clinical evaluation

Each patient underwent an endoscopic examination performed by an experienced gastrointestinal physician, and the results were recorded. Based on a comprehensive evaluation of the endoscopy results and clinical symptoms (such as hematemesis, bloody stool, and black stool), 116 patients who had never experienced EVB were included in the non-bleeding group (non-EVB, including 30 patients with mild EV, 15 patients with moderate EV, and 71 patients with severe EV) and 92 patients in bleeding group. In addition, those who had EVB within 2 weeks before the contrast enhanced CT and endoscopy were included in the bleeding group (EVB, n = 92).

Contrast-enhanced CT examination

Detailed parameters of CT examination are shown in Supplementary Table 1. Each patient performed contrast-enhanced CT within two weeks prior to the endoscopy. Contrast medium (300 mg/mL) was administered intravenously with a high-pressure syringe at a flow rate of 2.5 mL/s. The total amount of contrast medium (2 mL/kg) was calculated based on the patient's body weight. Enhanced arterial, portal, and delayed phase images were obtained at 30 seconds, 70 seconds, and 120 seconds after injection, and portal phase images were preserved.

Region-of-interest segmentation

In this study, three region-of-interest (ROI) were selected: The whole liver, whole spleen, and lower esophagus–fundus region. The portal phase contrast enhanced CT images were imported using 3D-Slicer software and manually delineated layer-by-layer by two radiologists who were blinded to the patient's condition and who had 10 and 5 years of diagnostic expertise in abdominal CT imaging, respectively. Differences of opinion on the outline of the ROI were discussed and

decided upon by the two experts. The specific criteria were as follows: (1) Because the liver and spleen are parenchymatous organs, the delineation should be as close to the edge of the organs as possible while avoiding the interference from other organs, including the kidney, intestine, gallbladder, and large blood vessels around the hilum of the liver and spleen; and (2) The sketch of the lower esophagus–gastric fundus region should include varicose veins, which are located 5 cm above the heart, as this is the most common site of EV[1]. Simultaneously, we tried to avoid space in the cavity and eliminate interference from food residue and air in the cavity. After 1 month, 30 patients were randomly selected, and the aforementioned ROI delineation was independently repeated by radiologists 1 and 2 without knowledge of the patient's condition to calculate the inter-observer correlation coefficients (ICC) and intra-observer ICC of radiomic features. The radiomic features with high consistency and repeatability were selected by calculating ICC values, which helped reduce experimental errors and subjectivity in manual ROI segmentation.

Radiomic features extraction and selection

Radiomic features were extracted using 3D-Slicer software. First, all images were preprocessed *via* image resampling, image grayscale quantization, Gaussian filtering, and wavelet filtering. Then, the collected feature values were normalized using the Z-score to remove dimensional disparities. To prevent the risk of model overfitting, the following steps were taken during feature selection: (1) Features with intra and inter-observer ICC > 0.8 for all the three ROIs were selected to ensure the stability of features; and (2) The most reliable and effective features were chosen using the least absolute shrinkage and selection operator (LASSO) regression analysis.

Collection of clinical data

Data were collected on clinical variables for each patient: Age, sex, etiology of cirrhosis, ascites, hypertension, PVT, Child–Pugh grade, alpha-fetoprotein, serum albumin, prothrombin time (PT), platelet, alanine transaminase (ALT), aspartate transaminase (AST), glutamyl transpeptidase, total bilirubin, direct bilirubin, and indirect bilirubin. These data are retrieved from the electronic medical records system.

Model construction and validation

Based on the radiomic features that the training cohort selected, the radiomic score (Rad-score) was constructed. The Rad-score was the predicted value determined by a linear combination weighted by the chosen radiomic features and matching LASSO regression coefficients (the radiomics model). Since our research was based on three ROIs (liver, spleen, and esophagus) to extract radiomics features, we planned to establish six different prediction models: (1) Rad-score (liver) based on the extracted radiomic features of the liver and its coefficients; (2) Rad-score (spleen) based on the extracted radiomic features of the spleen and its coefficients; (3) Rad-score (esophagus) based on the extracted radiomic features of the esophagus and its coefficients; (4) Rad-score (liver + spleen + esophagus), a radiomic fusion model based on the radiomic features extracted from the three ROIs of the liver, spleen, and esophagus; (5) Clinical model containing only independent clinical risk factors analyzed from the patient's clinical data; and (6) Radiomics-clinical model (RC model), a new radiomics-clinical combined model combining the Rad-score (liver + spleen + esophagus) and clinical model. Each of these six different predictive models could be used to predict EVB risk in patients with cirrhosis. In addition, we evaluated and compared the predictive performances of these six models using the validation cohort. The area under the receiver operating characteristic (ROC) curve (AUC) was used to evaluate model discrimination. The sensitivity, specificity, accuracy, positive predictive value (PPV), and negative predictive value (NPV) of each model were calculated, and different models were compared by the Delong test. The degree of model calibration was evaluated by calibration curve, and its clinical utility was evaluated using a decision curve. To make the RC model more intuitive, it was presented as a nomogram. The detailed research process is presented in Figure 2.

Statistical analysis

Statistical analysis was conducted using SPSS (Version 26.0; IBM) and Open-Source R software (Version 4.4.2; https://www.rproject.org). Bilateral P values < 0.05 were considered statistically significant. The χ^2 test or Fisher's exact test was used to examine classification factors expressed as percentages. An independent samples t-test was used to evaluate continuous data that followed a normal distribution and were expressed as the mean ± SD. The Mann-Whitney U test was used to assess continuous variables with non-normal distributions that were expressed as medians (range). The open-source software R was used to construct and validate the model.

RESULTS

Study population

This study included 208 patients with liver cirrhosis who were randomly assigned to the training (n = 145) and validation (n = 63) cohorts. The baseline data and clinical parameters of all patients are shown in Table 1. No clinical factor showed a significant difference between the training and validation cohorts (P > 0.05).

Selection of radiomic features

Each ROI yielded 1316 features in total. For each patient, 3948 features were retrieved. The inter-observer ICC averages of the liver, spleen, and lower esophagus–gastric fundus region were 0.828, 0.846, and 0.837, respectively, and the intra-observer ICC averages were 0.844, 0.831, and 0.827, respectively, which indicated that the outlined ROI had good con-

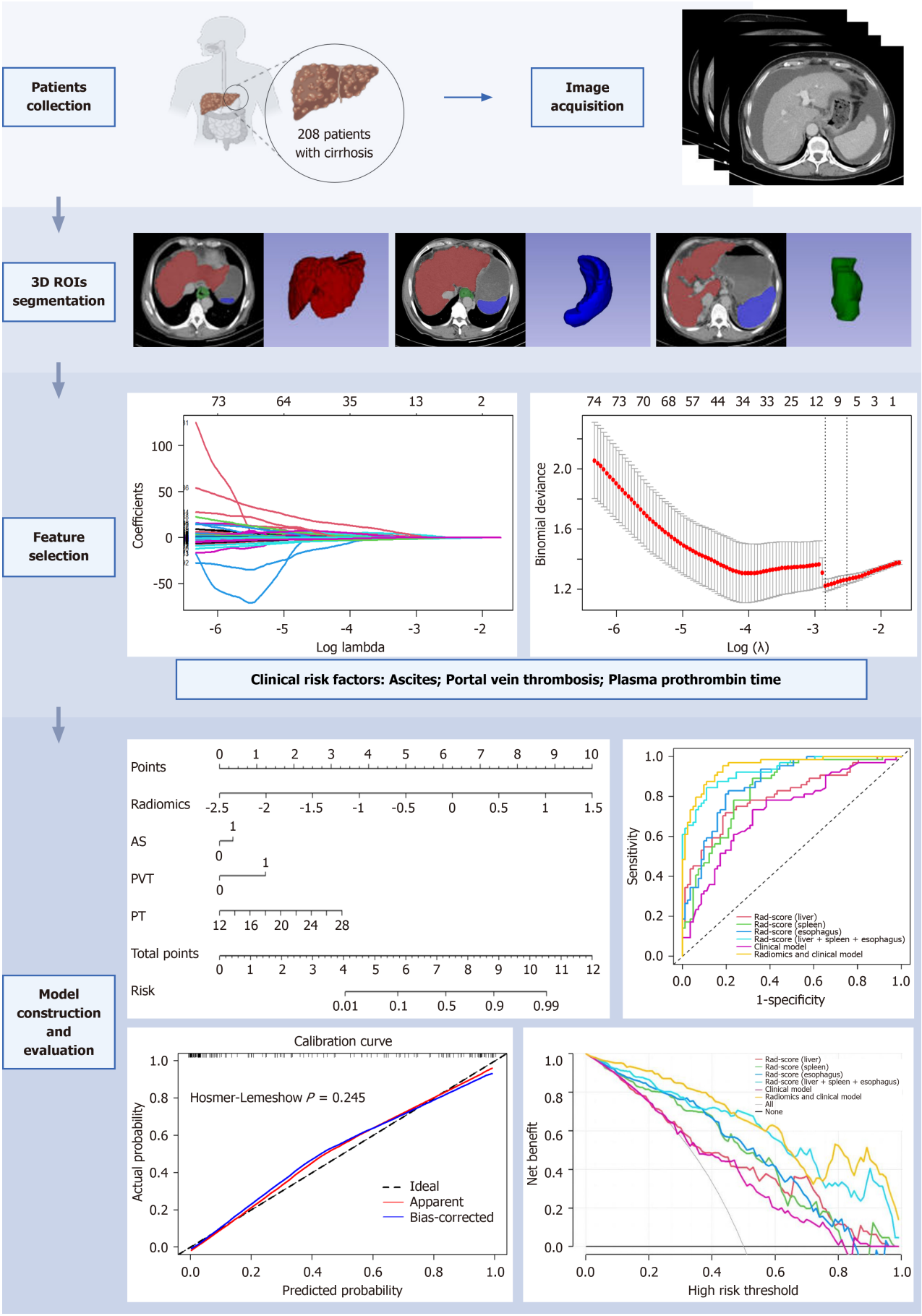

Figure 2 Radiomics workflow. ROI: Region-of-interest.

Table 1 Clinical characteristics of the patients, *n* (%)

Characteristics	Training cohort (*n* = 145)	Validation cohort (*n* = 63)	*P* value
Age (years)	54.6 ± 11.6	54.3 ± 13.8	0.869
Sex			0.250
Male	82 (56.6)	41 (65.1)	
Female	63 (43.4)	22 (34.9)	
Etiology			0.112
HBV	95 (65.5)	44 (69.8)	
Alcohol	18 (12.4)	1 (1.6)	
PBC	9 (6.2)	4 (6.3)	
AIH	5 (3.4)	1 (1.6)	
HCV	2 (1.4)	2 (3.2)	
HLD	2 (1.4)	1 (1.6)	
Other	14 (9.7)	10 (15.9)	
Ascites			0.624
Absent	66 (45.5)	31 (49.2)	
Present	79 (54.5)	32 (50.8)	
Hypertension			0.149
Absent	129 (89.0)	60 (95.2)	
Present	16 (11.0)	3 (4.8)	
PVT			0.175
Absent	118 (81.4)	46 (73)	
Present	27 (18.6)	17 (27)	
Child-Pugh			0.629
Class A	55 (37.9)	27 (42.9)	
Class B	68 (46.9)	25 (39.7)	
Class C	22 (15.2)	11 (17.5)	
AFP (μg/L)			0.772
< 20	122 (84.1)	54 (85.7)	
≥ 20	23 (15.9)	9 (14.3)	
ALB (g/L), mean ± SD	34.5 ± 6.0	33.5 ± 6.0	0.271
PT (second), median (range)	16.1 (14.9-17.5)	15.8 (14.7-17.4)	0.480
PLT (109/L), median (range)	54.0 (41.0-73.5)	57.0 (43.0-84.0)	0.395
ALT (U/L), median (range)	28.0 (19.5-50.0)	31.0 (21.0-57.0)	0.362
AST (U/L), median (range)	42.0 (29.5-69.0)	45.0 (29.0-73.0)	0.754
GGT (U/L), median (range)	44.0 (24.0-97.5)	44.0 (24.0-97.0)	0.953
TBIL (μmol/L), median (range)	28.0 (20.4-44.1)	23.1 (18.3-43.9)	0.226
DBIL (μmol/L), median (range)	10.0 (6.9-16.4)	9.1 (6.4-16.8)	0.712
IBIL (μmol/L), median (range)	17.8 (11.7-27.3)	14.9 (10.3-22.5)	0.076

HBV: Hepatitis B virus; PBC: Primary biliary cirrhosis; AIH: Autoimmune hepatitis; HCV: Hepatitis C virus; HLD: Hepatolenticular degeneration; PVT: Portal vein thrombosis; AFP: Alpha-fetoprotein; ALB: Serum albumin; PT: Prothrombin time; PLT: Platelet count; ALT: Alanine aminotransferase; AST: Aspartate aminotransferase; GGT: Glutamyl transpeptidase; TBIL: Total bilirubin; DBIL: Direct bilirubin; IBIL: Indirect bilirubin.

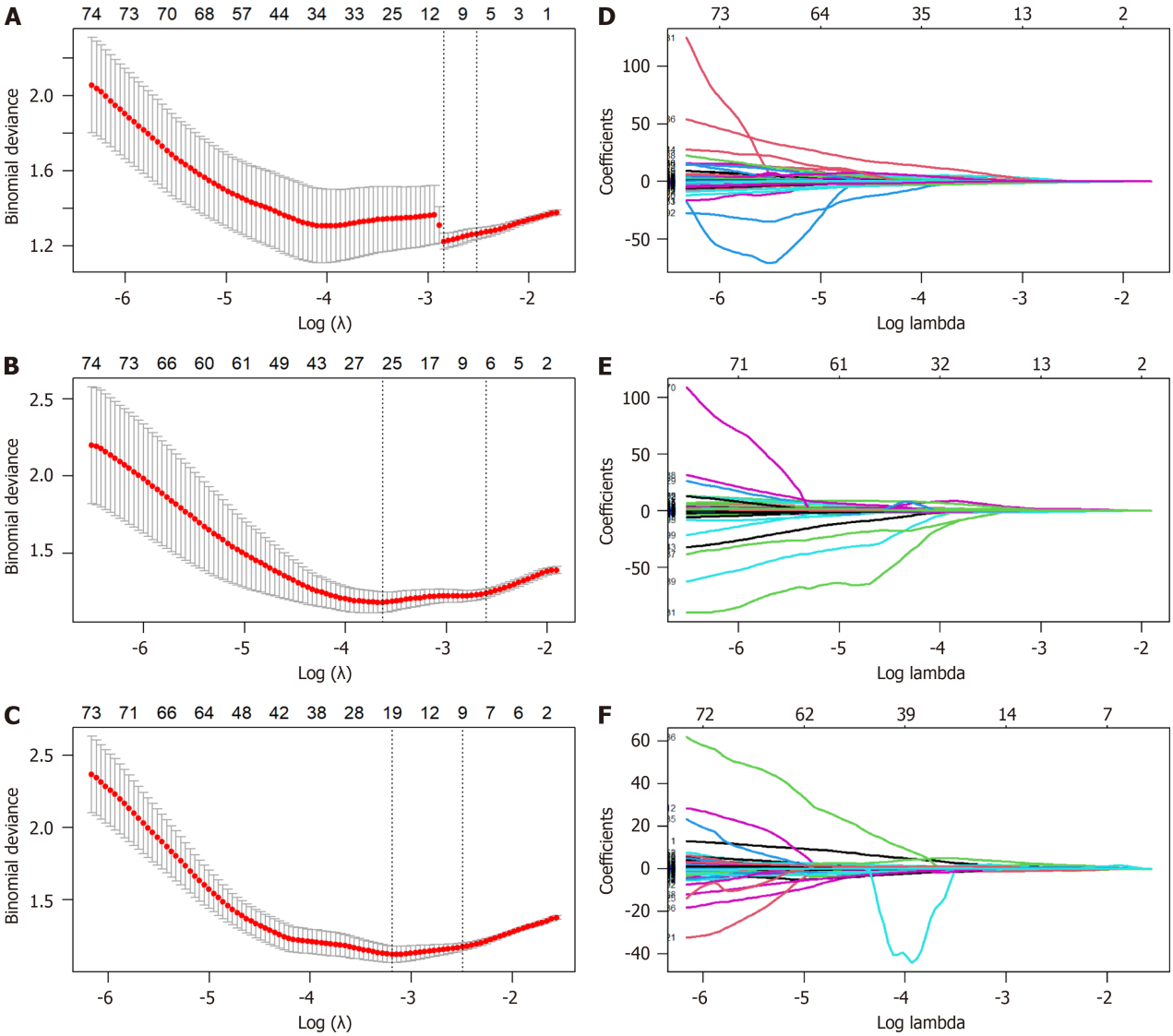

Figure 3 The process of feature selection and dimensionality reduction through least absolute shrinkage and selection operator. A-C: Least absolute shrinkage and selection operator regression model cross-verifies the selection process of the penalty parameter Lambda, and selects the radiomic features with non-zero coefficients according to the principle of minimum deviation; D-F: Convergence diagram of radiomic feature coefficients.

sistency and repeatability. Therefore, the radiomics features with ICCs greater than 0.8 were chosen from the three ROIs.

Through LASSO regression analysis, six features were selected from the liver (Figure 3A, Supplementary Table 2), six from the spleen (Figure 3B, Supplementary Table 3), and nine from the lower esophagus-gastric fundus region (Figure 3C, Supplementary Table 4). A total of 15 radiomic features (including four features of the liver, four features of the spleen, and seven features of the lower esophagus-gastric fundus) were selected from the established radiomics fusion model (liver + spleen + esophagus) (Figure 3D-F). The corresponding Rad-score was calculated (Supplementary Table 5), which was also used to establish the RC model, which is a new combined predictive model based on the Rad-score (liver + spleen + esophagus) and independent clinical risk factors.

Analysis of clinical risk factors

Univariate logistic regression analysis indicated that five factors were significantly correlated with first-instance secondary EVB in patients with cirrhosis: Ascites, PVT, PT, ALT, and AST (Table 2). Multivariate analysis revealed that ascites, PVT, and PT were independent clinical predictors for first-instance secondary EVB in patients with cirrhosis (Table 2).

Model construction and evaluation

Three independent clinical risk factors (ascites, PVT, and PT) were used to construct independent clinical prediction models. The Rad-score (liver + spleen + esophagus) was added to the above model to construct a nomogram using multivariable logistic regression analysis, resulting in the RC model. Figure 4 shows the nomogram for the RC model. The AUC, sensitivity, specificity, accuracy, PPV, and NPV values were used to evaluate the discriminative abilities of different models (Tables 3 and 4). The RC model yielded the best predictive performance, with AUC values in the training and validation cohorts of 0.951 [95% confidence interval (CI): 0.919-0.983] and 0.930 (95%CI: 0.872-0.987), respectively, which

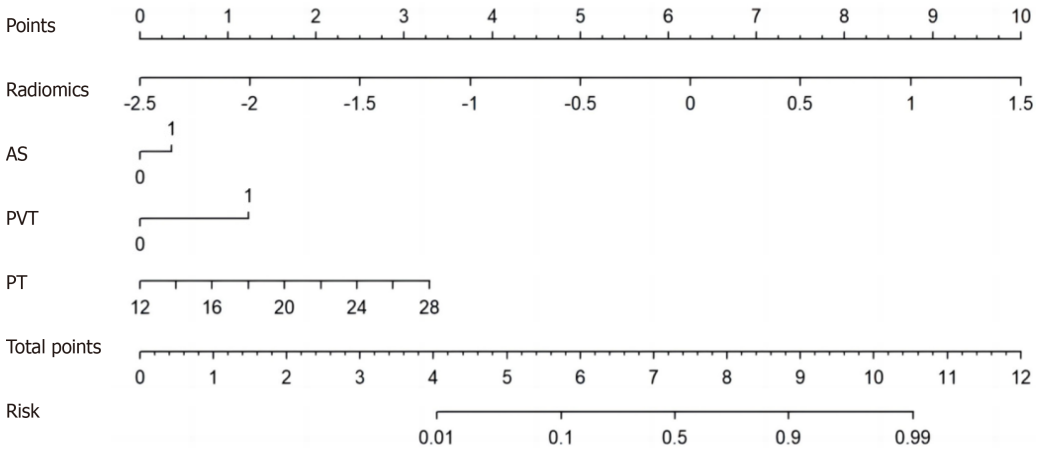

Figure 4 Nomogram for the radiomics-clinical model. Radiomics, Rad-score (liver + spleen + esophagus). AS: Ascites; PVT: Portal vein thrombosis; PT: Prothrombin time.

were close to those for the Rad-score (liver + spleen + esophagus) [AUC: 0.930 (95%CI: 0.891-0.970) and 0.886 (95%CI: 0.808-0.964)], respectively, and higher than those for the independent radiomics and independent clinical models.

According to the independent radiomics model, the AUC values of the Rad-score (esophagus) in the training [0.864 (95%CI: 0.807-0.922)] and validation [0.857 (95%CI: 0.762-0.952)] cohorts were slightly higher than those of the Rad-score (liver) [0.801 (95%CI: 0.727-0.875) and 0.763 (95%CI: 0.646-0.880), respectively] and Rad-score (spleen) [0.831 (95%CI: 0.766-0.897) and 0.792 (95%CI: 0.677-0.906), respectively]; the AUC values of the Rad-score (liver) and Rad-score (spleen) were similar. Figure 5A shows the ROC curves of different models. The outcomes of DeLong test comparison between each model and the RC model are displayed in Table 3.

The calibration curve was combined with Hosmer-Lemeshow test to evaluate the calibration of RC model. The results for the training (P = 0.245) and validation (P = 0.738) cohorts showed no significant difference (P > 0.05) between the predicted and real values of the RC model; the fitness of RC model was good. Figure 5B shows the calibration curve for the RC model. The prediction curves were close to the standard curve, which indicated that the prediction probability of cirrhotic EVB risk obtained using the RC model was in good agreement with the actual probability of occurrence. The net benefit of each model was analyzed using decision curves (Figure 5C). According to the decision curve analysis results, the net benefit of the RC model was the highest, and within a certain threshold range, the net benefit of the RC model was very close to that of the Rad-score (liver + spleen + esophagus) and Rad-score (esophagus).

DISCUSSION

Multi-organ radiomics analyses are essential for predicting EVB in the context of cirrhosis, allowing for the extraction of more complete/comprehensive information. We conducted a comprehensively radiomics analysis that included three ROIs for the whole liver, whole spleen, and lower esophagus-gastric fundus to establish six non-invasive models for predicting the risk of the first secondary EVB in patients with cirrhosis. In addition, the current study compared the prediction performance of a single-organ model, multi-organ model, and independent clinical model separately and in combination. The results indicated that the RC model combining radiomic fusion features and clinical characteristics yielded the best predictive performance, indicating a further improvement in diagnostic performance. The probability of EVB predicted by the RC model was very close to that of actual occurrence, and the net clinical benefit was the largest for the RC model.

The RC model contains 15 radiomics features related to EVB prediction, including four features from the liver, four features from the spleen, and seven features from the esophagogastric fundus region. The main features in the RC model were extracted from the esophagogastric fundus region, meaning that the radiomics features of this region have a great advantage in EVB prediction. The main features include one shape feature, five features of the first order, and nine features of texture. The surface volume ratio shape feature is a 3D feature, which was negatively correlated with EVB, indicating that the smaller the value, the higher the risk of bleeding. The first-order features include the median and kurtosis. The median can reflect the uniformity of the measured voxels, whereas kurtosis is a measure of signal strength distribution in ROI images. The more complex the structure of the tissue, the higher the kurtosis[21]. In this study, Kurtosis positively correlated with the risk of EVB, meaning that the higher the kurtosis, the higher the risk of bleeding. Texture features include second-order and high-order features, including three features of gray level run length matrix, two features of gray level co-occurrence matrix, two features of gray level dependence matrix, and two features of gray-level size zone matrix, which can extract the texture information of multi-domain and multi-scale images. Therefore, the subtle changes in the internal structure of the organs of patients with cirrhosis can be reflected, and different tissue structures can be quantitatively described and distinguished to provide biological information that cannot be observed by human eye[22-24].

Table 2 Univariate and multivariable analysis of clinical variables

Variables	Univariate logistic regression		Multivariable logistic regression	
	OR (95%CI)	*P* value	OR (95%CI)	*P* value
Age	1.000 (0.978-1.022)	0.973		
Sex	1.677 (0.959-2.932)	0.070		
Etiology	1.008 (0.880-1.154)	0.905		
Ascites	2.826 (1.597-5.001)	< 0.001	2.625 (1.367-5.039)	0.004
Hypertension	0.690 (0.268-1.775)	0.441		
PVT	4.622 (2.215-9.645)	< 0.001	3.500 (1.547-7.916)	0.003
Child-Pugh	1.352 (0.916-2.007)	0.130		
AFP	0.977 (0.457-2.088)	0.953		
ALB	0.965 (0.921-1.011)	0.135		
PT	1.158 (1.032-1.299)	0.013	1.199 (1.033-1.390)	0.017
PLT	0.999 (0.992-1.007)	0.832		
ALT	0.978 (0.966-0.991)	0.001		
AST	0.982 (0.973-0.992)	0.001		
GGT	0.998 (0.995-1.001)	0.136		
TBIL	0.996 (0.988-1.005)	0.405		
DBIL	0.994 (0.981-1.008)	0.427		
IBIL	0.995 (0.977-1.012)	0.546		

PVT: Portal vein thrombosis; AFP: Alpha-fetoprotein; ALB: Serum albumin; PT: Prothrombin time; PLT: Platelet count; ALT: Alanine aminotransferase; AST: Aspartate aminotransferase; GGT: Glutamyl transpeptidase; TBIL: Total bilirubin; DBIL: Direct bilirubin; IBIL: Indirect bilirubin.

Table 3 Area under the receiver operating characteristic curve values of different models in training and validation cohorts

Models	Training cohort		Validation cohort	
	AUC (95%CI)	*P* value	AUC (95%CI)	*P* value
Rad-score (liver)	0.801 (0.727-0.875)	< 0.001	0.763 (0.646-0.880)	0.002
Rad-score (spleen)	0.831 (0.766-0.897)	< 0.001	0.792 (0.677-0.906)	0.016
Rad-score (esophagus)	0.864 (0.807-0.922)	< 0.001	0.857 (0.762-0.952)	0.109
Rad-score (liver+ spleen + esophagus)	0.930 (0.891-0.970)	0.049	0.886 (0.808-0.964)	0.139
Clinical model	0.727 (0.644-0.811)	< 0.001	0.692 (0.556-0.828)	< 0.001
RC model	0.951 (0.919-0.983)		0.93 (0.872-0.987)	

P value is the results of Delong test between each model and the RC model. AUC: Area under the receiver operating characteristic curve; RC model: Radiomics-clinical model.

Among the three independent radiomic models, the Rad-score (esophagus) had the best predictive ability, indicating that the radiomic features of the esophagogastric fundus region were more important. As this is the direct site of varices and bleeding, these results are consistent with clinical findings. The predictive performance of the Rad-score (spleen) was slightly higher than that of the Rad-score (liver), which may be because systemic hyperdynamic circulation is the main factor influencing the maintenance or aggravation of portal hypertension following development of the collateral circulation in patients with cirrhosis. This in turn can lead to splenomegaly, splenic congestion, and increased spleen hardness, reflecting extrahepatic hemodynamic changes[1]. Several studies have shown that spleen hardness is more important than liver hardness for the noninvasive prediction of esophageal and gastric varices in cirrhosis[25-27]. The Rad-score (liver + spleen + esophagus) performed much better in terms of prediction than the independent radiomics model, consistent with our hypothesis. The significance of the radiomics features and its weight coefficient in each model are consistent with the clinical pathophysiology of EVB. The effectiveness of the multi-organ combination model

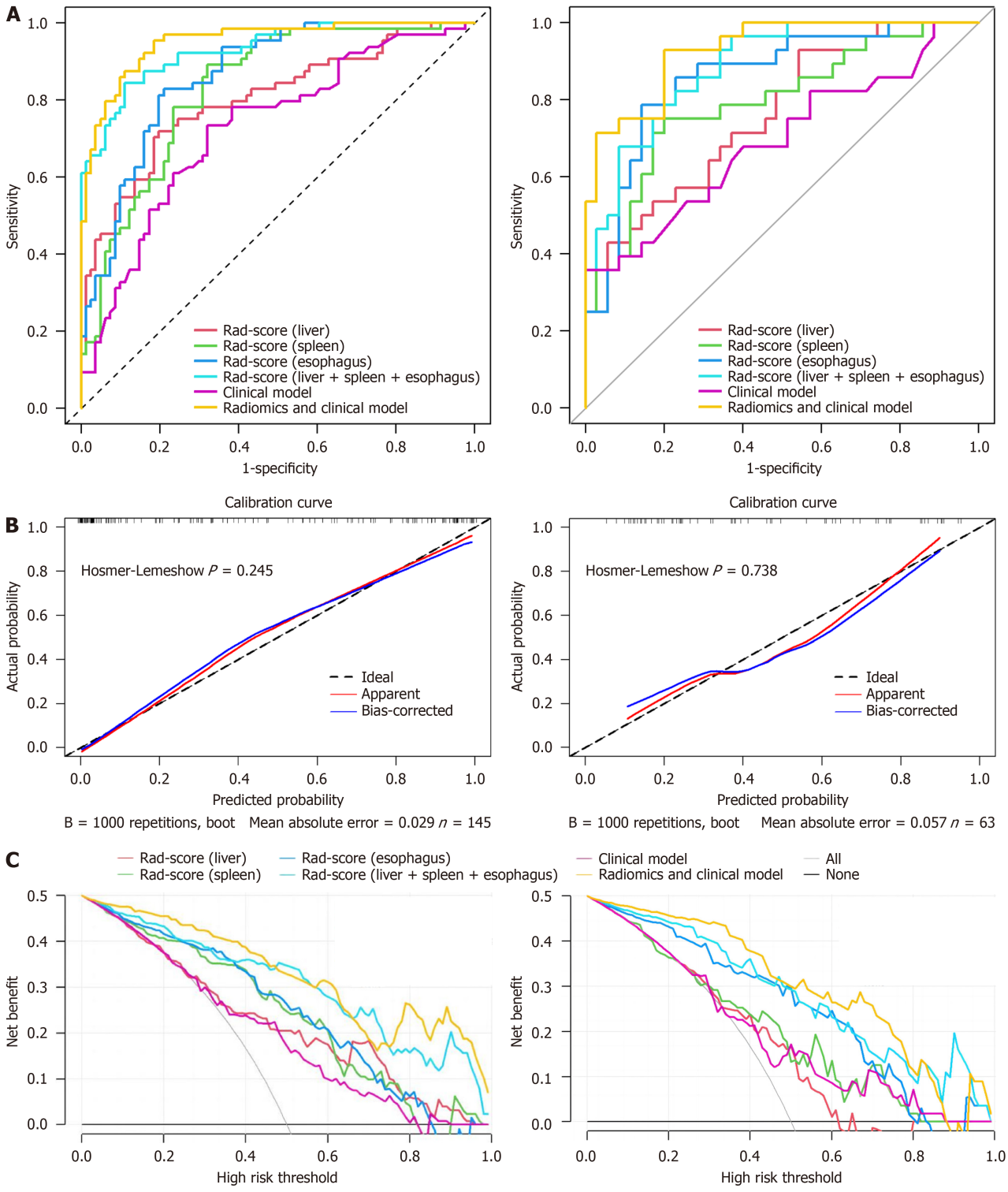

Figure 5 Model construction and evaluation. A: The receiver operating characteristic curves of each model in training (left) and validation (right) cohorts; B: The calibration curve of the radiomics-clinical model in training (left) and validation (right) cohorts; C: The decision curves of each model in training (left) and validation (right) cohorts.

established in this study is effective, and its stability has been verified.

The results of clinical data analyses indicated that ascites, PVT, and PT were independent clinical predictors of secondary EVB in patients with cirrhosis. Ascites is a manifestation of decompensation in patients with liver cirrhosis. Portal vein pressure increases during ascites formation, which leads to different degrees of EV, and EVB is a secondary event in severe cases[28,29]. Previous studies have already identified ascites as an independent risk feature for predicting secondary EVB in patients with cirrhosis[30-32], consistent with our findings. In addition, PVT not only increases portal hypertension, reduces portal blood flow, worsens liver function, and increases mortality in patients with liver cirrhosis, but also increases the risk of severe gastroesophageal varices, EV bleeding, and rebleeding[33,34]. This result is in line with the findings of earlier research[13,17]. Additionally, our research revealed that PT is an independent predictor of

Table 4 Evaluation of predictive performance in training and validation cohorts

Models	Cohort	Sensitivity	Specificity	Accuracy	PPV	NPV
Rad-score (liver)	Training	0.656	0.815	0.745	0.737	0.750
	Validation	0.643	0.686	0.667	0.621	0.706
Rad-score (spleen)	Training	0.750	0.765	0.759	0.716	0.795
	Validation	0.714	0.829	0.778	0.769	0.784
Rad-score (esophagus)	Training	0.734	0.802	0.772	0.746	0.793
	Validation	0.786	0.857	0.825	0.815	0.833
Rad-score (liver + spleen + esophagus)	Training	0.844	0.852	0.848	0.818	0.873
	Validation	0.779	0.886	0.794	0.826	0.775
Clinical model	Training	0.531	0.790	0.676	0.667	0.687
	Validation	0.571	0.686	0.635	0.600	0.667
RC model	Training	0.875	0.877	0.876	0.848	0.899
	Validation	0.821	0.857	0.841	0.821	0.857

PPV: Positive predictive value; NPV: Negative predictive value; RC model: Radiomics-clinical model.

EVB in patients with cirrhosis, which may be due to a reduction or deficiency in the activity of synthetic plasma coagulation factors and the prolongation of PT[1]. Previous studies have demonstrated that PT prolongation is positively correlated with EV in patients with cirrhosis and that patients with portal hypertension are more likely to develop EVB [35,36]. However, the predictive performance of the clinical model in the training [AUC: 0.727 (95%CI: 0.644-0.811)] and validation [AUC: 0.692 (95%CI: 0.556-0.828)] cohorts was poor, possibly owing to the small sample size and/or selection bias.

Previous studies on radiomics for predicting EVB in cirrhosis have focused primarily on extracting the features only a portion of the liver and/or portions of the spleen or esophagus and outlining ROIs at single or multiple levels and some studies lack clinical data, without a comprehensive or complete analysis[13-17]. Our study has the following advantages. Our findings emphasize that segmentation resulting in multi-organ ROIs yields better predictive performance. Our model also included clinical factors from a patient cohort to ensure a comprehensive analysis. Although the traditional independent clinical model had poor prediction performance, the RC model combined with clinical risk factors and radiomics fusion features showed the best predictive performance. Additionally, the RC model was more efficient than the Rad-score (liver + spleen + esophagus), demonstrating that clinical risk factors are essential for predicting EVB, consistent with the results of previous studies[13-15]. These clinical laboratory indicators can quickly and intuitively assess the EVB risk of patients with cirrhosis, while the RC model can be used to noninvasively and quantitatively predict the risk of EVB.

Although our study is a single-center study with a small sample size, we studied patients with HBV and other etiologies. In the non-bleeding group, 30 patients had mild EV, 15 patients had moderate EV, and 71 patients had severe EV. Thus, this study was not limited to a certain category of patients, but included a rather broad population, which is important for generalizing the results. Most importantly, we segmented the 3D model of multiple organs, which is more comprehensive and complete than that in previous studies.

However, our study has some limitations. First, the sample size was relatively small, and the current research results are based on single-center data. The results may differ from that of participants in different regions and institutions. We should expand the sample size in the future, conduct multi-center, large-sample research, and include an external validation set to further confirm the applicability of the research results. Second, there is no unified standard and method for automatic segmentation of ROI, which should be explored in the future.

CONCLUSION

Our model combining radiomic features from multi-organ portal-phase contrast enhanced CT images with clinical risk factors can be used for the noninvasive prediction of EVB risk in patients with cirrhosis.

FOOTNOTES

Author contributions: Peng YJ designed research, performed research, analyzed data and wrote the paper; Liu X performed research and analyzed data; Liu Y contributed analytic tools; Tang X data acquisition; Zhao QP data acquisition; Du Y designed research, project

administration and making critical revisions. All authors read and agreed to the published version of the manuscript.

Institutional review board statement: This study was approved by the institutional review board of the Affiliated Hospital of North Sichuan Medical College (IRB-2022ER432-1).

Informed consent statement: This study was approved by the institutional review board of the Affiliated Hospital of North Sichuan Medical College and the requirement for patient-informed consent was waived for this retrospective analysis.

Conflict-of-interest statement: All authors declare no conflict of interest.

Data sharing statement: No additional data are available.

Country of origin: China

ORCID number: Yong Du 0000-0002-8119-3195.

S-Editor: Qu XL
L-Editor: A
P-Editor: Xu ZH

REFERENCES

1 **Ginès P**, Krag A, Abraldes JG, Solà E, Fabrellas N, Kamath PS. Liver cirrhosis. *Lancet* 2021; **398**: 1359-1376 [PMID: 34543610 DOI: 10.1016/S0140-6736(21)01374-X]
2 **Asrani SK**, Devarbhavi H, Eaton J, Kamath PS. Burden of liver diseases in the world. *J Hepatol* 2019; **70**: 151-171 [PMID: 30266282 DOI: 10.1016/j.jhep.2018.09.014]
3 **GBD 2017 Cirrhosis Collaborators**. The global, regional, and national burden of cirrhosis by cause in 195 countries and territories, 1990-2017: a systematic analysis for the Global Burden of Disease Study 2017. *Lancet Gastroenterol Hepatol* 2020; **5**: 245-266 [PMID: 31981519 DOI: 10.1016/S2468-1253(19)30349-8]
4 **Yoshiji H**, Nagoshi S, Akahane T, Asaoka Y, Ueno Y, Ogawa K, Kawaguchi T, Kurosaki M, Sakaida I, Shimizu M, Taniai M, Terai S, Nishikawa H, Hiasa Y, Hidaka H, Miwa H, Chayama K, Enomoto N, Shimosegawa T, Takehara T, Koike K. Evidence-based clinical practice guidelines for Liver Cirrhosis 2020. *J Gastroenterol* 2021; **56**: 593-619 [PMID: 34231046 DOI: 10.1007/s00535-021-01788-x]
5 **European Association for the Study of the Liver**. EASL Clinical Practice Guidelines on prevention and management of bleeding and thrombosis in patients with cirrhosis. *J Hepatol* 2022; **76**: 1151-1184 [PMID: 35300861 DOI: 10.1016/j.jhep.2021.09.003]
6 **Biggins SW**, Angeli P, Garcia-Tsao G, Ginès P, Ling SC, Nadim MK, Wong F, Kim WR. Diagnosis, Evaluation, and Management of Ascites, Spontaneous Bacterial Peritonitis and Hepatorenal Syndrome: 2021 Practice Guidance by the American Association for the Study of Liver Diseases. *Hepatology* 2021; **74**: 1014-1048 [PMID: 33942342 DOI: 10.1002/hep.31884]
7 **Huang DQ**, Terrault NA, Tacke F, Gluud LL, Arrese M, Bugianesi E, Loomba R. Global epidemiology of cirrhosis - aetiology, trends and predictions. *Nat Rev Gastroenterol Hepatol* 2023; **20**: 388-398 [PMID: 36977794 DOI: 10.1038/s41575-023-00759-2]
8 **Meng D**, Wei Y, Feng X, Kang B, Wang X, Qi J, Zhao X, Zhu Q. CT-Based Radiomics Score Can Accurately Predict Esophageal Variceal Rebleeding in Cirrhotic Patients. *Front Med (Lausanne)* 2021; **8**: 745931 [PMID: 34805214 DOI: 10.3389/fmed.2021.745931]
9 **Wan S**, Wei Y, Zhang X, Liu X, Zhang W, He Y, Yuan F, Yao S, Yue Y, Song B. Multiparametric radiomics nomogram may be used for predicting the severity of esophageal varices in cirrhotic patients. *Ann Transl Med* 2020; **8**: 186 [PMID: 32309333 DOI: 10.21037/atm.2020.01.122]
10 **Jakab SS**, Garcia-Tsao G. Evaluation and Management of Esophageal and Gastric Varices in Patients with Cirrhosis. *Clin Liver Dis* 2020; **24**: 335-350 [PMID: 32620275 DOI: 10.1016/j.cld.2020.04.011]
11 **Park HJ**, Park B, Lee SS. Radiomics and Deep Learning: Hepatic Applications. *Korean J Radiol* 2020; **21**: 387-401 [PMID: 32193887 DOI: 10.3348/kjr.2019.0752]
12 **Sung YS**, Park B, Park HJ, Lee SS. Radiomics and deep learning in liver diseases. *J Gastroenterol Hepatol* 2021; **36**: 561-568 [PMID: 33709608 DOI: 10.1111/jgh.15414]
13 **Yang JQ**, Zeng R, Cao JM, Wu CQ, Chen TW, Li R, Zhang XM, Ou J, Li HJ, Mu QW. Predicting gastro-oesophageal variceal bleeding in hepatitis B-related cirrhosis by CT radiomics signature. *Clin Radiol* 2019; **74**: 976.e1-976.e9 [PMID: 31604574 DOI: 10.1016/j.crad.2019.08.028]
14 **Lin Y**, Li L, Yu D, Liu Z, Zhang S, Wang Q, Li Y, Cheng B, Qiao J, Gao Y. A novel radiomics-platelet nomogram for the prediction of gastroesophageal varices needing treatment in cirrhotic patients. *Hepatol Int* 2021; **15**: 995-1005 [PMID: 34115257 DOI: 10.1007/s12072-021-10208-4]
15 **Gao Y**, Yu Q, Li X, Xia C, Zhou J, Xia T, Zhao B, Qiu Y, Zha JH, Wang Y, Tang T, Lv Y, Ye J, Xu C, Ju S. An imaging-based machine learning model outperforms clinical risk scores for prognosis of cirrhotic variceal bleeding. *Eur Radiol* 2023; **33**: 8965-8973 [PMID: 37452878 DOI: 10.1007/s00330-023-09938-w]
16 **Yan Y**, Li Y, Fan C, Zhang Y, Zhang S, Wang Z, Huang T, Ding Z, Hu K, Li L, Ding H. A novel machine learning-based radiomic model for diagnosing high bleeding risk esophageal varices in cirrhotic patients. *Hepatol Int* 2022; **16**: 423-432 [PMID: 35366193 DOI: 10.1007/s12072-021-10292-6]

17 **Luo R**, Gao J, Gan W, Xie WB. Clinical-radiomics nomogram for predicting esophagogastric variceal bleeding risk noninvasively in patients with cirrhosis. *World J Gastroenterol* 2023; **29**: 1076-1089 [PMID: 36844133 DOI: 10.3748/wjg.v29.i6.1076]

18 **Lam SK**, Zhang Y, Zhang J, Li B, Sun JC, Liu CY, Chou PH, Teng X, Ma ZR, Ni RY, Zhou T, Peng T, Xiao HN, Li T, Ren G, Cheung AL, Lee FK, Yip CW, Au KH, Lee VH, Chang AT, Chan LW, Cai J. Multi-Organ Omics-Based Prediction for Adaptive Radiation Therapy Eligibility in Nasopharyngeal Carcinoma Patients Undergoing Concurrent Chemoradiotherapy. *Front Oncol* 2021; **11**: 792024 [PMID: 35174068 DOI: 10.3389/fonc.2021.792024]

19 **Le VH**, Kha QH, Minh TNT, Nguyen VH, Le VL, Le NQK. Development and Validation of CT-Based Radiomics Signature for Overall Survival Prediction in Multi-organ Cancer. *J Digit Imaging* 2023; **36**: 911-922 [PMID: 36717518 DOI: 10.1007/s10278-023-00778-0]

20 **Tang O**, Xu Y, Tang Y, Lee HH, Chen Y, Gao D, Han S, Gao R, Savona MR, Abramson RG, Huo Y, Landman BA. Validation and Optimization of Multi-Organ Segmentation on Clinical Imaging Archives. *Proc SPIE Int Soc Opt Eng* 2020; **11313** [PMID: 34040277 DOI: 10.1117/12.2549035]

21 **Al-Hasani M**, Sultan LR, Sagreiya H, Cary TW, Karmacharya MB, Sehgal CM. Machine learning improves early detection of liver fibrosis by quantitative ultrasound radiomics. *IEEE Int Ultrason Symp* 2022; **2022** [PMID: 37220606 DOI: 10.1109/ius54386.2022.9957180]

22 **Sack J**, Nitsch J, Meine H, Kikinis R, Halle M, Rutherford A. Quantitative Analysis of Liver Disease Using MRI-Based Radiomic Features of the Liver and Spleen. *J Imaging* 2022; **8** [PMID: 36286371 DOI: 10.3390/jimaging8100277]

23 **Wu Z**, Matsui O, Kitao A, Kozaka K, Koda W, Kobayashi S, Ryu Y, Minami T, Sanada J, Gabata T. Hepatitis C related chronic liver cirrhosis: feasibility of texture analysis of MR images for classification of fibrosis stage and necroinflammatory activity grade. *PLoS One* 2015; **10**: e0118297 [PMID: 25742285 DOI: 10.1371/journal.pone.0118297]

24 **Wan S**, Wei Y, Zhang X, Yang C, Hu F, Song B. Computed Tomography-Based Texture Features for the Risk Stratification of Portal Hypertension and Prediction of Survival in Patients With Cirrhosis: A Preliminary Study. *Front Med (Lausanne)* 2022; **9**: 863596 [PMID: 35433759 DOI: 10.3389/fmed.2022.863596]

25 **Ma X**, Wang L, Wu H, Feng Y, Han X, Bu H, Zhu Q. Spleen Stiffness Is Superior to Liver Stiffness for Predicting Esophageal Varices in Chronic Liver Disease: A Meta-Analysis. *PLoS One* 2016; **11**: e0165786 [PMID: 27829057 DOI: 10.1371/journal.pone.0165786]

26 **Sharma P**, Kirnake V, Tyagi P, Bansal N, Singla V, Kumar A, Arora A. Spleen stiffness in patients with cirrhosis in predicting esophageal varices. *Am J Gastroenterol* 2013; **108**: 1101-1107 [PMID: 23629600 DOI: 10.1038/ajg.2013.119]

27 **Colecchia A**, Montrone L, Scaioli E, Bacchi-Reggiani ML, Colli A, Casazza G, Schiumerini R, Turco L, Di Biase AR, Mazzella G, Marzi L, Arena U, Pinzani M, Festi D. Measurement of spleen stiffness to evaluate portal hypertension and the presence of esophageal varices in patients with HCV-related cirrhosis. *Gastroenterology* 2012; **143**: 646-654 [PMID: 22643348 DOI: 10.1053/j.gastro.2012.05.035]

28 **Chinese Society of Hepatology, Chinese Medical Association**, Xu X, Duan Z, Ding H, Li W, Jia J, Wei L, Linghu E, Zhuang H. Chinese guidelines on the management of ascites and its related complications in cirrhosis. *Hepatol Int* 2019; **13**: 1-21 [PMID: 30656520 DOI: 10.1007/s12072-018-09923-2]

29 **Rudler M**, Mallet M, Sultanik P, Bouzbib C, Thabut D. Optimal management of ascites. *Liver Int* 2020; **40** Suppl 1: 128-135 [PMID: 32077614 DOI: 10.1111/liv.14361]

30 **Zhang Q**, Niu S, Yang L, Zhu B, Shi K, Zhang X, Zhang Y, Bi Y, Mu Y, Wang X. A novel prognostic model for predicting the risk of first variceal hemorrhage in patients with HBV-related cirrhosis. *Front Cell Infect Microbiol* 2023; **13**: 1062172 [PMID: 36733609 DOI: 10.3389/fcimb.2023.1062172]

31 **North Italian Endoscopic Club for the Study and Treatment of Esophageal Varices**. Prediction of the first variceal hemorrhage in patients with cirrhosis of the liver and esophageal varices. A prospective multicenter study. *N Engl J Med* 1988; **319**: 983-989 [PMID: 3262200 DOI: 10.1056/NEJM198810133191505]

32 **El Sheref SEDM**, Afify S, Berengy MS. Clinical characteristics and predictors of esophagogastric variceal bleeding among patients with HCV-induced liver cirrhosis: An observational comparative study. *PLoS One* 2022; **17**: e0275373 [PMID: 36227871 DOI: 10.1371/journal.pone.0275373]

33 **Senzolo M**, Garcia-Tsao G, García-Pagán JC. Current knowledge and management of portal vein thrombosis in cirrhosis. *J Hepatol* 2021; **75**: 442-453 [PMID: 33930474 DOI: 10.1016/j.jhep.2021.04.029]

34 **Xu DQ**, Yang JH. [Correlational study on portal vein thrombosis of liver cirrhosis]. *Zhonghua Gan Zang Bing Za Zhi* 2020; **28**: 573-579 [PMID: 32791792 DOI: 10.3760/cma.j.cn501113-20190404-00107]

35 **Islam MN**, Khan M, Ahmad N, Mamun-Al-Mahtab, Karim MF. Plasma Prothrombin Time and Esophageal Varices in Patients with Cirrhosis of Liver. *Euroasian J Hepatogastroenterol* 2016; **6**: 10-12 [PMID: 29201717 DOI: 10.5005/jp-journals-10018-1158]

36 **Ruberto MF**, Marongiu F, Sorbello O, Civolani A, Demelia L, Barcellona D. Are prothrombin time and clot waveform analysis useful in detecting a bleeding risk in liver cirrhosis? *Int J Lab Hematol* 2019; **41**: 118-123 [PMID: 30298976 DOI: 10.1111/ijlh.12934]

Published by **Baishideng Publishing Group Inc**
7041 Koll Center Parkway, Suite 160, Pleasanton, CA 94566, USA
Telephone: +1-925-3991568
E-mail: office@baishideng.com
Help Desk: https://www.f6publishing.com/helpdesk
https://www.wjgnet.com